Polymer Journal (2012) 44, 155–161

www.nature.com/pj

ORIGINAL ARTICLE

Kinetics of coarsening in immiscible poly(ε-caprolactone)/poly(styrene-*co*-acrylonitrile) blends

Lenka Jelínková[1], Petr Svoboda[2], Petr Sáha[1] and Takashi Inoue[3]

The morphological development of immiscible blends of poly(ε-caprolactone) (PCL) and poly(styrene-*co*-acrylonitrile) (SAN) during static annealing was studied using time-resolved light scattering and optical microscopy. In the melt-blended samples, coarsening was not observable at low temperatures, even above the glass transition temperature of SAN (T_g=113 °C). It occurred when a critical temperature *T (for example, 170 °C for a PCL/SAN (50/50) blend) was reached. *T** was found to have a strong dependence on the blend composition, and we suggest that this results from an effect of the large difference in viscosities of pure PCL and SAN on the particle collision rate. The morphological development of solution-prepared blends was found to differ greatly from that of the melt-blended samples. At first, spinodal decomposition (SD) began, and then collision kinetics prevailed over SD. After the particles grew to a size of approximately 10 μm, secondary SD took place and small domains (~1 μm) appeared in both the matrix and the particles. Consequently, the overall coarsening behavior varied significantly from the predictions of current theories.**
Polymer Journal (2012) **44,** 155–161; doi:10.1038/pj.2011.110; published online 26 October 2011

Keywords: coarsening; polymer blend; poly(ε-caprolactone); poly(styrene-*co*-acrylonitrile)

INTRODUCTION

Polymer blends have a widespread range of technological applications. As such, these materials have been the subject of many investigations, particularly, with respect to their processing behavior in the two-phase state.[1–4]

When an immiscible polymer pair is mixed in the molten state, a dispersed phase/matrix morphology, with either droplets or fibers as the dispersed phase, or a co-continuous morphology with two interlocking halves can be formed.[5] Within the composition range $\phi_i \pm \Delta\phi$, the roles of two liquids invert: the dispersed liquid becomes continuous and vice versa.[1] The condition for phase inversion is expressed by:

$$\phi_1/\phi_2 = \eta_1/\eta_2, \quad (1)$$

where ϕ_i is the volume fraction and η_i is the viscosity of component i.[6–8] Other parameters that control the morphology of polymer blends are the interfacial tension and elasticity of the components.[9]

The morphology of multiphase materials, that is, the size, shape and distribution of the blend components, is generally sensitive to process variables (for example, stress, temperature, pressure and residence time) and a sophisticated line control is required, compared with single-phase polymers.[2–4] The key is the stability of the morphology, or in other words, of the size of the dispersed particles, during the processing step. Flow also has an important role in the structure of the processed material and forms a flow-induced morphology.[3,10–12] The flow-induced morphology strongly depends on the blend composition, the components aspect ratio and also the stress field. Already at very low concentrations ($\phi_i > 0.02$), solid particles preferentially combine into doublets, while liquid drops undergo a continuous process of dispersion and coalescence.

In the melt of an immiscible polymer blend, coarsening is defined as the growth of the particle size with annealing time to reduce the interfacial free energy. The effect begins with random motion of isolated dispersed particles, that is, clusters or droplets, as Brownian-like particles. If two such particles collide, they coalesce into a larger one. In this case, the growth law of the particle size negligibly depends on surface tension.[13] Ostwald ripening (evaporation–condensation), collision–coalescence and hydrodynamic mechanisms have been used to explain this coarsening behavior.

Ostwald ripening[14] concerns the kinetics of 'evaporation' of molecules from small particles and their 'condensation' to larger particles. The driving force for the process is described by the curvature dependence of the chemical potential:[15]

$$\mu = \mu_0 + V_m \gamma \kappa, \quad (2)$$

where μ is the chemical potential at a flat interface, V_m is the molar volume, γ is the interfacial energy and κ is the interfacial curvature of the particles.

The collision–coalescence mechanism[16] concerns the Brownian motion of dispersed particles. In this theory, particles collide with

[1]Centre of Polymer Systems, Polymer Centre, Tomas Bata University in Zlín, Zlín, Czech Republic; [2]Centre of Polymer Systems, Department of Polymer Engineering, Tomas Bata University in Zlín, Zlín, Czech Republic and [3]Department of Polymer Science and Engineering, Yamagata University, Yonezawa, Japan
Correspondence: Dr L Jelínková, Centre of Polymer Systems, Polymer Centre, Tomas Bata University in Zlín, TGM 5555, Zlín 760 01, Czech Republic.
E-mail: jelinkova@uni.utb.cz
Received 6 May 2011; revised 1 September 2011; accepted 7 September 2011; published online 26 October 2011

one another to decrease the total free energy of the system. Both the evaporation–condensation and the collision–coalescence mechanisms yield the same time dependence:

$$r^3 = r_0^3 = Kt. \tag{3}$$

The cube of the average particle radius r^3 increases linearly with annealing time t, starting from an initial value r_0^3 at time $t=0$. K is the proportionality constant related to the coarsening, which depends on the temperature and volume fraction of the particles.

The hydrodynamic flow mechanism explains the morphological development of a bicontinuous two-phase system. In this mechanism, the domain size d increases linearly with time:[17]

$$d \sim (\gamma/\eta)t. \tag{4}$$

Several experimental studies have investigated the coarsening behavior in immiscible polymer blend.[11,12,18–24] A few studies concern the coarsening behavior of two-phase systems composed of dispersed particles in a matrix.[11, 12, 18–21]

With the growing concern for the environment, the biodegradability of the poly(ε-caprolactone) (PCL)/ poly(styrene-*co*-acrylonitrile) (SAN) systems is becoming increasingly important for the plastic industry.[25,26] It is known that PCL and SAN are miscible only in a limited range of copolymer composition, that is, the blends display a window of miscibility in the temperature–copolymer composition plane (from ~8 to 28 wt % of acrylonitrile in SAN).[27–30] In this study, we chose immiscible PCL/SAN blends (SAN containing 35.2 wt % of AN) and investigated the kinetics of the coarsening behavior during static annealing at different temperatures using light scattering and optical microscopy. To investigate the morphological development over a wide range of initial particle size D, not only melt-blending but also solution-blending (with ensuing precipitation) was performed to study the difference in coarsening behavior between these variously prepared blends.

EXPERIMENTAL PROCEDURE

For the PCL, a commercial polymer from the Union Carbide Corp., a subsidiary of the Dow Chemical Company, Danbury, CT, USA (TONE 767 E, M_w=40 400 g mol^{-1}, M_w/M_n=2.61, T_m=61 °C, T_g=−60 °C) was selected. SAN containing 35.2 wt % of acrylonitrile (SAN-36; Luran 378 P, M_w=88 200 g mol^{-1}, M_w/M_n=2.1, T_g=113 °C) was obtained from BASF SE, Ludwigshafen, Germany.

The PCL was melt-mixed with 30, 50 and 70 wt % of SAN. The melt-mixing was carried out in a miniature mixer (Mini-Max Moulder, Model CS-183 MMX, Custom Scientific Instruments Inc., Easton, PA, USA) at 200 °C for 7 min with a rotor speed of 100 min^{-1}. The extruded melt was quickly quenched into dry ice-methanol (−73 °C) to freeze the two-phase structure in the melt. The solution cast method was also used to prepare PCL/SAN blends containing 30, 50 and 70 wt % of SAN. PCL and SAN-36 were dissolved at 5 wt % of total polymer in 1, 2-dichloroethane. The solution was poured into methanol, resulting in immediate precipitation. The solvents were allowed to evaporate for 5 min at 60 °C and then for 24 h at room temperature.

The coarsening was analyzed using a time-resolved light-scattering apparatus and optical microscope equipped with a hot stage as follows.

A small piece of the quenched or precipitated specimen was placed between two pieces of cover glass and melt-pressed into a thin film (~20 μm thick) at a desired temperature (110–200 °C) for annealing on a hot stage set on a light-scattering apparatus. Immediately after melt-pressing, the melt specimen was subjected to the time-resolved measurement of the scattering profile (the angular dependence of the scattered light intensity). Radiation from a 632.8-nm-wavelength He-Ne laser was applied vertically to the film specimen. The intensity of the scattered light from the film was measured under the optical alignment of parallel polarization. The angular distribution of the scattered light intensity was detected by a CCD camera. The scattering profiles in time slices of 0.3 s were recorded at different time intervals in the range of 2 to 30 min during isothermal annealing and stored in a computer (OptiPlex XM 590 Dell, Pentium processor, Intel inside) equipped with Dyna-100 software for further analysis.

For the optical microscopy observation of the coarsening behavior, the quenched or precipitated specimen was quickly melt-pressed into a thin film on a hot stage at the desired temperature (110–200 °C). The melted specimen was immediately placed onto the hot-stage (TH 600) of the microscope. The structural development during the isothermal temperature in the range of 110–200 °C was observed under both an optical and also a polarizing microscope (Olympus BH-2, Olympus Optical, Co., Ltd., Tokyo, Japan) equipped with an exposure control unit (Olympus PM-20) and an Olympus camera.

The average particle size D of 300 particles was determined from an optical micrograph using ImageJ image-analyzing software.[31] The number-mean diameter D_n was calculated based on the real particle-size distribution from:[32]

$$D_n = \frac{\sum_i n_i D_i}{\sum_i n_i}, \tag{5}$$

where n_i is the number of particles having diameter D_i.

The rheological characteristics of the polymers were studied on a Rheoflixer capillary rheometer (SWO Polymertechnik GmbH, Krefeld, Germany) at constant piston speed, which was increased in a stepwise manner. The dies had a diameter of 1 mm and length-to-diameter (L/D) ratios of 10 and 20, and the capillary had a plane (90°) entrance. The experiments were performed at temperatures of 100–150 °C for PCL and 170–200 °C for SAN. The polymers were heated to a desired measuring temperature inside the rheometer barrel for at least 5 min before extrusion. The pressure in the cylinder was measured at the entrance region of the die with a Dynisco transducer. The results of the rheological measurements were viscosity curves calculated from the values of the piston speed (shear rate) and the pressure drop in the capillary (shear stress). The Bagley and Rabinowitsch corrections were accounted for. Bagley plots were obtained by varying the length while keeping the diameters of the capillary and reservoir constant. The viscosity curves were then calculated from the values of shear viscosity η as a function of shear rate $\dot{\gamma}$.

RESULTS AND DISCUSSION

Light scattering is a convenient technique for the quantitative evaluation of coarsening kinetics. All specimens exhibited a monotonously decreasing light-scattering profile, that is, the intensity of the scattering light I decreased monotonously with increasing scattering angle θ. From such scattering profiles, a series of morphological parameters from a Debye–Bueche plot can be obtained, that is, the plot of $I(q)^{-1/2}$ versus q^2, where q is the magnitude of the scattering vector given by $q=(4\pi/\lambda')\sin(\theta/2)$. Here, λ' is the wavelength of the light in the specimen.[33] When the plots are linear, the correlation distance ξ is given by the slope and intercept of the $I(q)^{-1/2}$ axis by:

$$I(q)^{-1/2} = (8\pi \langle \eta^2 \rangle \xi^3)^{-1/2}(1+\xi^2 q^2), \tag{6}$$

where $\langle \eta^2 \rangle$ is the mean-square fluctuation of the refractive index. Once the value of ξ is given, other morphological parameters, such as the specific interfacial area S_{sp} and the mean diameter of dispersed particles D, are obtained using:

$$S_{sp} = 4\phi(1-\phi)/\xi, \tag{7}$$

$$D = 6\phi/S_{sp}, \tag{8}$$

where ϕ is the volume fraction of the dispersed phase. The diameter of dispersed particles D thus obtained is then plotted as a function of annealing time.

In Figure 1, the examples of D vs annealing time plots are shown for the blends after melt-mixing at 100 min^{-1} for 7 min at 200 °C. Figures

1a and b are the results for the blend composition PCL/SAN-36 (70/30) at two different annealing temperatures: 110 and 200 °C. At 110 °C (Figure 1a), there is no change in diameter D, that is, no coarsening occurs even at the long time-scale of 12 h. It is important to note that the T_g of SAN is just above this temperature, which means that at this temperature, still rather hard droplets of SAN are unable to merge. For this blend composition containing a majority of PCL, the increase in particle size with annealing occurred at 130 °C, even though the process was very slow (within a 4 h time scale). We denote this onset temperature of coarsening by T^*. For annealing temperatures much higher than T^*, coarsening occurred at a faster rate. An example of fast coarsening is shown in Figure 1b at 200 °C. The kinetics seems to follow equation (4). At lower temperatures, the values were so scattered that it was sometimes difficult to judge whether the coarsening behavior followed equations (3) or (4). The reason for such large scattering is not obvious at present.

For the 50/50 PCL/SAN blend (Figure 1c), coarsening did not begin even at 150 °C. The T^* for the 50/50 blend was approximately 170 °C. Further, the 30/70 PCL/SAN blend did not show any appreciable change in diameter even at 200 °C, as shown in Figure 1d. The T^* was above 200 °C. T^* thus strongly depends on the blend composition; the smaller the amount of SAN, the lower the T^*.

Figure 2 shows the morphologies of melt-mixed 70/30 and 50/50 PCL/SAN blends after annealing at 200 °C and 170 °C, which are representative of the coarsened morphology via collision and collapse into bigger particles, resulting in a rather wide distribution of particle size (approximately 1–20 μm).

Quantitatively, the size D distribution of the dispersed SAN-36 particles using image analysis of Figure 2a in the melt-mixed PCL/SAN-36 (70/30) blend after 40 min static annealing at 200 °C is plotted in Figure 3. Their mean D_n was then calculated as 2.3 μm using equation (5). This was performed to confirm that the average D, obtained by light scattering from equations (6)–(8) in Figure 1,

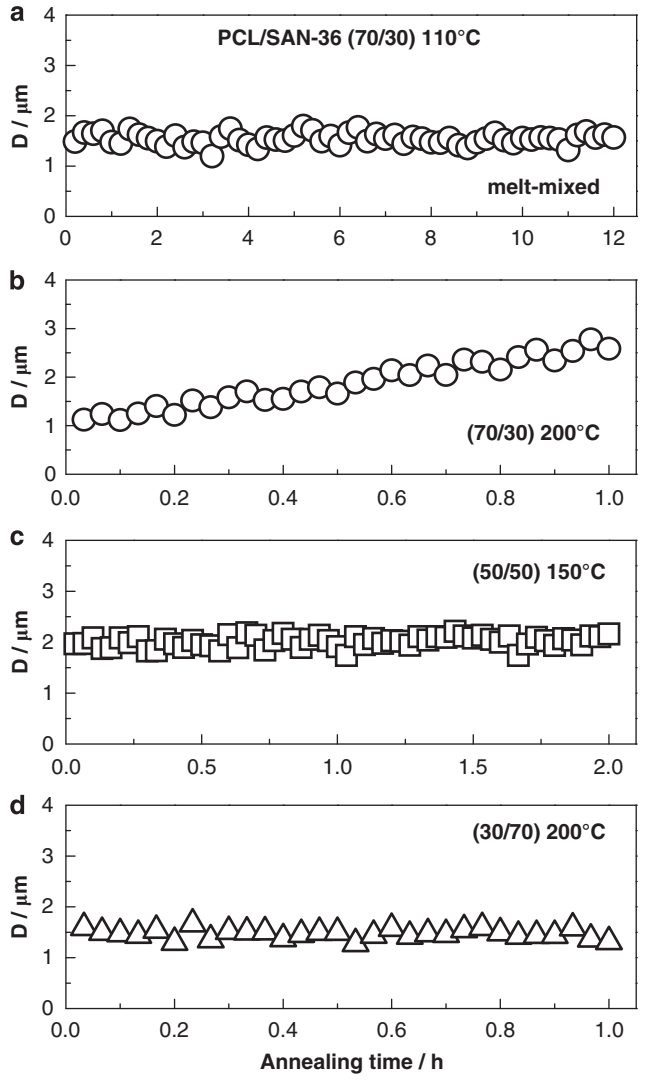

Figure 1 Time variation of the average particle size, D, by light scattering during static annealing after melt-mixing at 200 °C: PCL/SAN + annealing temperature: (**a**) 70/30 + 110 °C, (**b**) 70/30 + 200 °C, (**c**) 50/50 + 150 °C, (**d**) 30/70 + 200 °C.

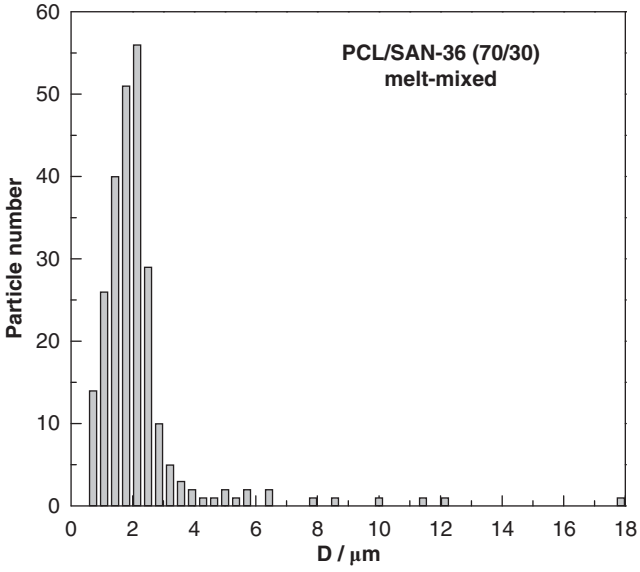

Figure 3 Number distribution of the particle size, D, by image analysis in melt-mixed PCL/SAN-36 (70/30) blend after 40 min static annealing at 200 °C.

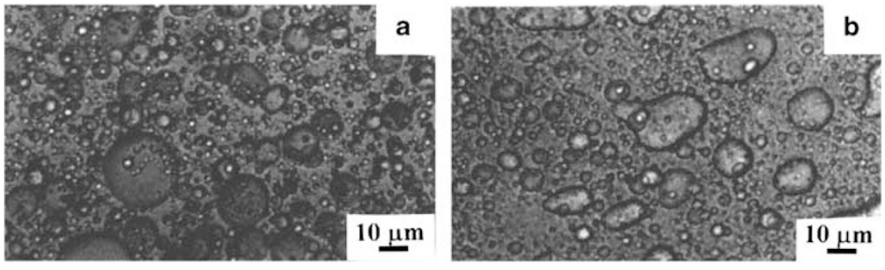

Figure 2 Optical micrographs of melt-mixed PCL/SAN-36 blends: (**a**) 70/30 after 40 min at 200 °C, (**b**) 50/50 after 2 h at 170 °C.

correctly corresponds to the average D shown in the optical micrographs in Figure 2.

To discuss the composition dependence of T^*, the results of the shear viscosity measurements are shown in Figures 4 and 5. Note that due to the large difference in the T_m of PCL (61 °C) and the T_g of SAN (113 °C), it was not possible to measure their viscosities at the same temperature range. SAN had much higher shear viscosity and shear thinning than PCL. Its viscosity curve showed nonlinear behavior, a steep linear negative slope, at all values of shear rates. As shown in Figure 5, there is a large gap between the viscosity (ca. 2 decades) between PCL and SAN at all measured temperatures. This difference may explain the composition dependence of T^*. In a PCL-rich system, the matrix viscosity is rather low even at lower annealing temperatures, so that the SAN particles can move by Brownian motion and merge after collision. In a SAN-rich system, the mobility of the PCL particles should be much lower in the high viscosity matrix so that the T^* would occur at much higher temperatures, at which Brownian motion becomes vigorous. Thus, the composition dependence of T^* may suggest that the collision process is rate-determining for the overall coarsening rate.

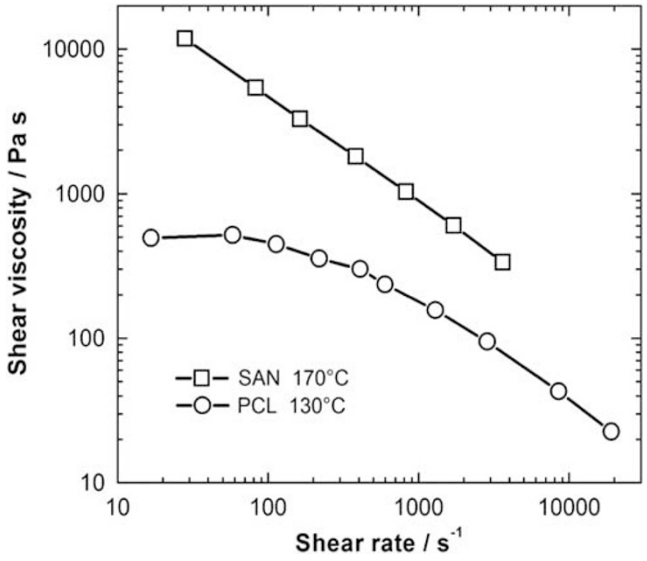

Figure 4 Shear viscosity vs shear rate for pure PCL at 130 °C and pure SAN at 170 °C.

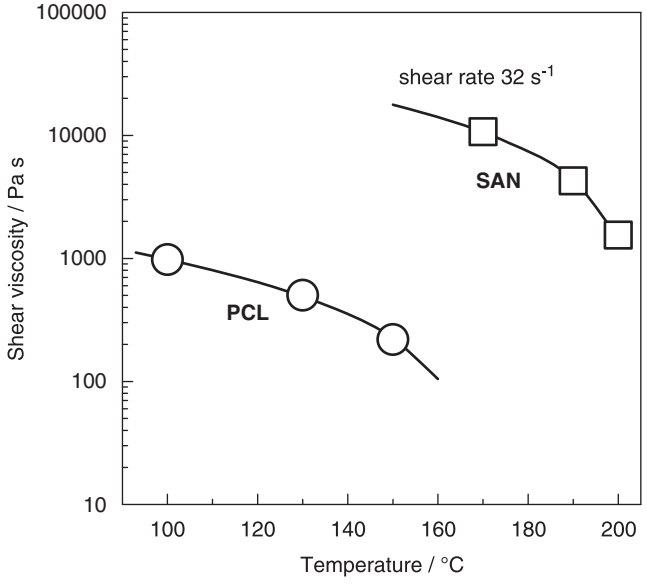

Figure 5 Shear viscosity vs temperature for pure PCL and pure SAN at a fixed shear rate of 32 s^{-1}.

The coarsening kinetics of the solution-prepared 70/30 PCL/SAN blend at 200 and 170 °C observed by light scattering are shown in Figure 6. According to the light-scattering data, the particles grow from the initial particle size of approximately 0.4 μm. We expected much smaller particle size or a nearly homogeneous state for the as-precipitated sample. However, it seems that a coarsening structure was formed in a few seconds during melt-pressing at 200 °C between the two pieces of cover glass (in advance of the light-scattering measurement). At 200 °C, the kinetics of coarsening is faster than at 170 °C. For both temperatures, fast growth is observed from the beginning and is followed by a plateau. At 170 °C, the particle size reaches a maximum and then starts to decrease. This strange behavior is much different from the kinetics predicted by equations (3) and (4) and could be interpreted using the following optical microscopy observations.

The coarsening behavior at 200 °C observed by optical microscopy is shown in Figure 7. At the beginning, a very fine and regular morphology with poor contrast is observed. Then the contrast is improved and the structure grows very quickly. The regularly phase-separated structure in Figures 7a and b should be achieved by spinodal decomposition (SD). The melt-pressing of the as-precipitated sample seems to cause the orientation of the structure. The memory of melt-pressing remains for a few minutes and then completely disappears after 6 min (Figure 7c). Anyhow, the structure in Figures 7a and b may correspond to the intermediate stage of SD.

After 6 min (Figure 7c), the structure has coarsened to particles of approximately 10 μm in size in a matrix. By annealing further, the particles grow to several tens of microns (Figure 7d). The photo in Figure 7e is a polarized optical micrograph of the quenched PCL/SAN (70/30) sample after annealing for 15 min. A crystalline texture is observed inside the large particles. Therefore, the large dispersed particles can be assigned to a PCL-rich region, and it seems that once the SAN forms a continuous phase, it is hard to destroy it because of its high viscosity in the molten-state, even though it is the minor component (at 30 wt%).

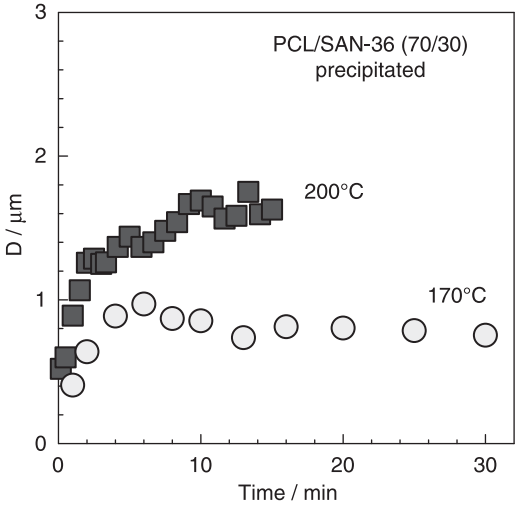

Figure 6 Time variation of the average particle size, D, of a PCL/SAN (70/30) blend prepared by precipitation into methanol, by light scattering, during static annealing at 200 °C and at 170 °C.

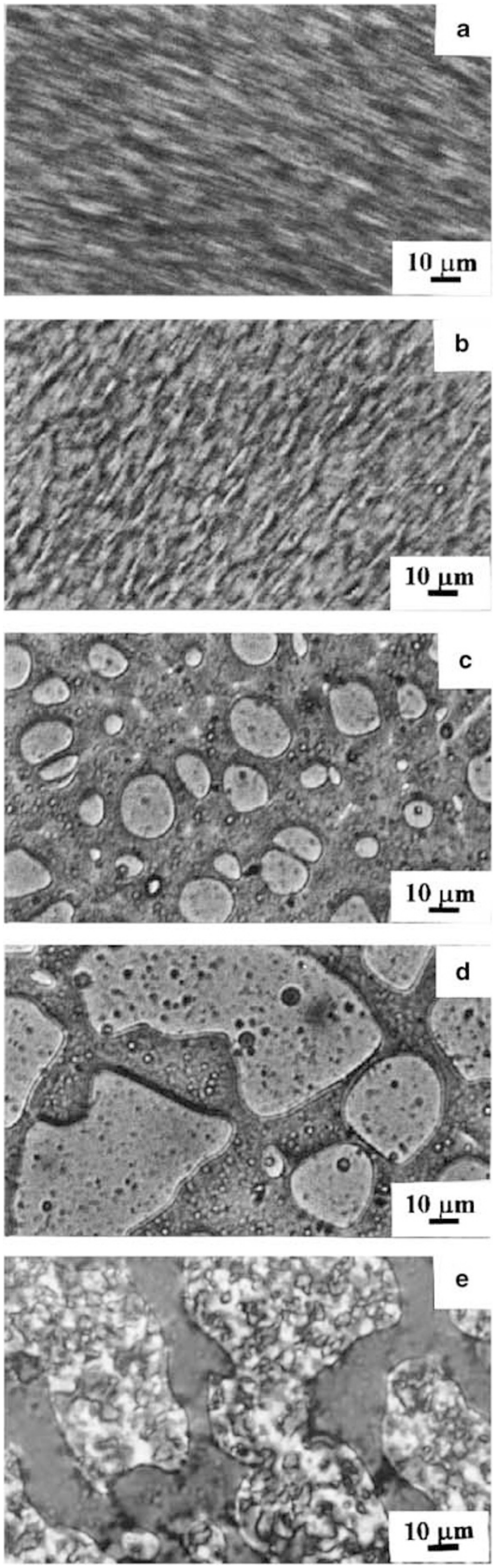

Figure 7 Optical micrographs of a PCL/SAN (70/30) blend prepared by precipitation into methanol, during static annealing at 200 °C: (**a**) after 1 min, (**b**) 2 min, (**c**) 6 min, (**d**) 15 min; (**e**) 15 min + quenched to 25 °C and crystallized.

Furthermore, one can also observe small domains of approximately 1–2 μm in size in both the PCL-rich and SAN-rich regions in Figure 7c. By annealing further, the number of small domains increases (Figure 7d). Light scattering is not concerned with the heterogeneity of several tens of microns but mostly with the concentration fluctuation caused by the appearance of small domains. That is, the appearance of small domains in both the particles and matrix may render the leveling-off of particle coarsening by light scattering observed in Figure 6.

The appearance of small domains could be explained as follows. If SD proceeds to reach droplet morphology and then the coalescence starts very quickly by mutual collision, the droplet size could increase

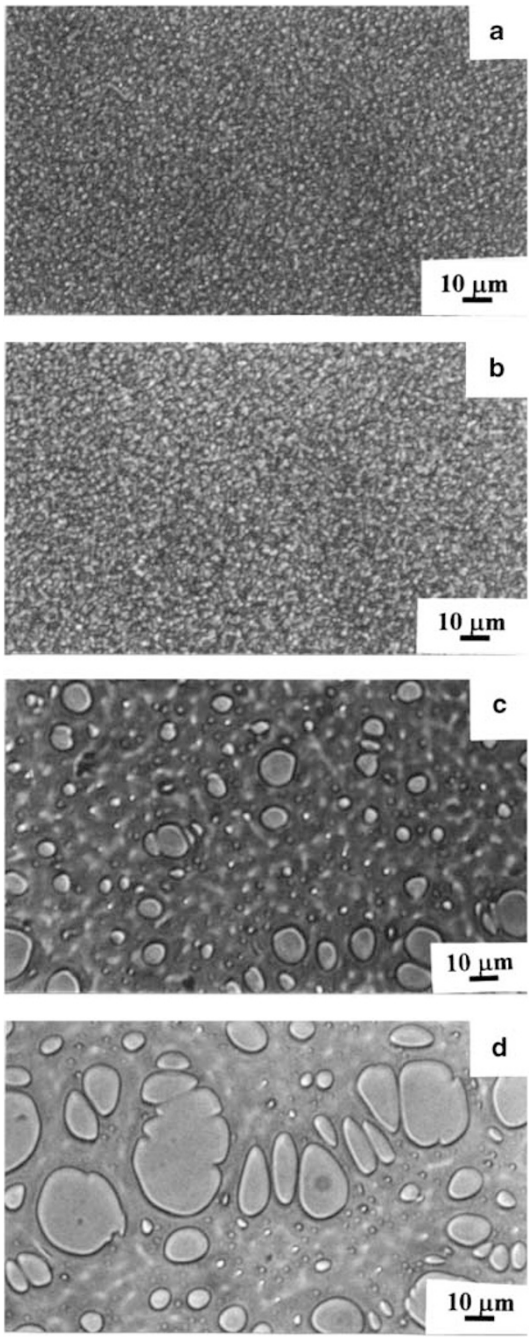

Figure 8 Optical micrographs of a PCL/SAN (70/30) blend prepared by precipitation into methanol, during static annealing at 170 °C: (**a**) after 1 min, (**b**) 6 min, (**c**) 40 min, (**d**) 60 min.

without a significant exchange of molecules; that is, without an appreciable change in the concentration of the PCL-rich and SAN-rich regions. That is, when coalescence prevails over the exchange of molecules by SD, a new SD could start in both regions to yield the small domains, because both regions are still on the way to approaching the coexisting compositions. Consequently, the coarsening kinetics may not follow the theory proposed by equations (3) and (4).

The structural development of the same blend at 170 °C is shown in Figure 8, and the situation seems to be similar to Figure 7. At this lower temperature, however, the coalescence occurs rather slowly (Figures 8c and d) and then, the second-step SD can proceed simultaneously to generate new concentration fluctuations with short wavelength in the matrix. Then, the average particle size by light scattering may start to decrease with time. Thus, also at this temperature, the coarsening seems to consist of two rate processes, SD and collision, so that the kinetics may be far from the theoretical predictions of equations (3) and (4).

The structural development of the solution-prepared 30/70 PCL/SAN blend at 170 °C is shown in Figure 9. The figure shows that coarsening occurred even at this lower temperature, whereas it did not occur in the melt-blended sample of the same composition at the same temperature. In the solution-prepared blend, the structural coarsening may begin via SD so that even when the droplet structure is formed (Figure 9b), the SAN-rich matrix could contain some amount of PCL. Then, collision would be possible for further coarsening. This phenomenon may explain the difference in coarsening behavior of the melt-blended sample, where the matrix consists of pure SAN.

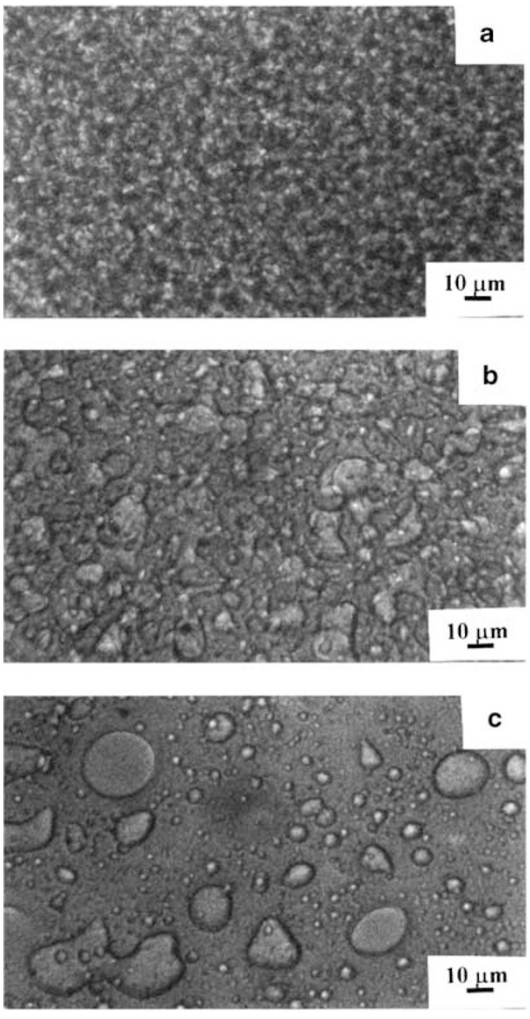

Figure 9 Optical micrographs of a PCL/SAN (30/70) blend prepared by precipitation into methanol, during static annealing at 170 °C: (**a**) after 10 min, (**b**) 40 min, (**c**) 120 min.

CONCLUSIONS

This paper describes the morphological development of an immiscible PCL/SAN blend during static annealing. In the case of melt-blended samples, coarsening begins at temperature T^* (above T_g of SAN) that depends strongly on blend composition. For 70/30 and 50/50 (PCL/SAN) compositions, T^* was found to be approximately 130 °C and 170 °C, respectively. At 200 °C, the increase in average particle size was linear with time. For the 30/70 blend, no coarsening was detected up to 200 °C.

The coarsening behavior of the solution-prepared blends was complicated. At first, SD started. Then, the growth proceeded by the collision of particles. After the particles grew to size of approximately 10 μm, the second step of SD began forming small domains (~ 1 μm in size) in both the matrix and large particles. The kinetics of coarsening observed by light scattering was very far from the theoretical predictions.

ACKNOWLEDGEMENTS

We are thankful for the support of the Operational Program Research and Development for Innovations co-funded by the European Regional Development Fund (ERDF) and national budget of the Czech Republic, within the framework of the Centre of Polymer Systems project (reg. number: CZ.1.05/2.1.00/03.0111), and also of the Ministry of Education, Youth and Sports of the Czech Republic (grant number: MSM 7088352101).

1 Utracki, L. A. *Polymer Alloys and Blends: Thermodynamics and Rheology*, Hanser Publishers, Munich, 1989.
2 Collyer, A. A. & Clegg, D. W. Eds *Rheological Measurements*, Elsevier Applied Sciences, London, 1988.
3 Utracki, L. A. *Two-Phase Polymer Systems*, Hanser Publishers, Munich, 1991.
4 Utracki, L. A. *Polymer Blends Handbook*, Vol. 1. Kluwer Academic Publishers, Dordrecht, 2002.
5 Gergen, W. P. Uniqueness of hydrogenated block copolymers for elastomer applications. *Kautschuk Gummi Kunststoffe* **37,** 284–290 (1984).
6 Jordhamo, G. M., Manson, J. A. & Sperling, L. H. Phase continuity and inversion in polymer blends and simultaneous interpenetrating networks. *Polym. Eng. Sci.* **26,** 517–524 (1986).
7 Paul, D. R. & Barlow, J. W. Polymer blends (or alloys). *J. Macromol. Sci. Rev. Macromol. Chem. Phys.* **C18,** 109–168 (1980).
8 Verhoogt, H. Morphology, properties and stability of thermoplastic polymer blends (Ph.D. thesis, Delft University of Technology, 1992).
9 Persson, L. A. Filler controlled morphology in polymer blends (Ph.D. thesis, Chalmers University of technology, 1997).
10 Das, N. C., Wang, H., Mewis, J. & Moldenaers, P. Rheology and microstructures formation of immiscible model polymer blends under steady state and transient flows. *J. Polym. Sci., Part B: Polym. Phys.* **43,** 3519–3533 (2005).
11 Hanafy, G. M., Madbouly, S. A., Ougizawa, T. & Inoue, T. Effect of shear history on the morphology and coarsening behaviour of polycarbonate/poly(styrene-co-acrylonitrile) blend. *Polymer* **46,** 705–712 (2005).
12 Filippone, G., Netti, P. A. & Acierno, D. Microstructural evolutions of LDPE/PA6 blends by rheological and rheo-optical analyses: influence of flow and compatibilizer on break-up and coalescence processes. *Polymer* **48,** 564–573 (2007).
13 Araki, T., Tran-Cong, Q. & Shibayama, M. *Structure and Properties of Multiphase Polymeric Materials*, Marcel Dekker, Inc., New York, 1998.
14 Lifshitz, I. M. & Slyozov, V. V. The kinetics of precipitation from supersaturated solid solutions. *J. Phys. Chem. Solids* **19,** 35–50 (1961).
15 Wagner, C. Z. Theorie der Alterung von Niederschlagen durch Umlosen (Ostwald-Reifung). *Z. Elektrochem.* **65,** 581–591 (1961).
16 Binder, K. & Stauffer, D. Theory for slowing down of relaxation and spinodal decomposition of binary-mixtures. *Phys. Rev. Lett.* **33,** 1006–1009 (1974).
17 Siggia, E. D. Late stages of spinodal decomposition in binary-mixtures. *Phys. Rev. A* **20,** 595–605 (1979).
18 Crist, B. & Nesarikar, A. R. Coarsening in polyethylene copolymer blends. *Macromolecules* **28,** 890–896 (1995).

19 Mirabella, F. M. Phase-separation and the kinetics of phase coarsening in commercial impact polypropylene copolymers. *J. Polym. Sci., Part B: Polym. Phys.* **32,** 1205–1216 (1994).
20 Mirabella, F. M. & Barley, J. S. Ostwald ripening in an immiscible hydrogenated polybutadiene and high-density polyethylene blend. *J. Polym. Sci., Part B: Polym. Phys.* **32,** 2187–2195 (1994).
21 Chuang, W. T., Shih, K. S. & Hong, P. D. Kinetics of phase separation in poly (ε-caprolactone)/poly(ethylene glycol) blends. *J. Polym. Res.* **12,** 197–204 (2005).
22 Hill, M. J. & Barham, P. J. Ostwald ripening in polyethylene blends. *Polymer* **36,** 3369–3375 (1995).
23 Tanaka, H. New coarsening mechanisms for spinodal decomposition having droplet pattern in binary-fluid mixture - collision-induced collisions. *Phys. Rev. Lett.* **72,** 1702–1705 (1994).
24 Yuan, Z. H. & Favis, B. D. Coarsening of immiscible co-continuous blends during quiescent annealing. *AIChE J.* **51,** 271–280 (2005).
25 Choi, E. J. & Park, J. K. Study on biodegradability of PCL/SAN blend using composting method. *Polym. Degrad. Stab.* **52,** 321–326 (1996).
26 Cho, K., Lee, J. & Xing, P. X. Enzymatic degradation of blends of poly(ε-caprolactone) and poly(styrene-co-acrylonitrile) by pseudomonas lipase. *J. Appl. Polym. Sci.* **83,** 868–879 (2002).
27 Schulze, K., Kressler, J. & Kammer, H. W. Phase-behavior of poly(ε-caprolactone) poly(styrene-*ran*-acrylonitrile) blends exhibiting both liquid-liquid unmixing and crystallization. *Polymer* **34,** 3704–3709 (1993).
28 Svoboda, P., Keyzlarová, L., Sáha, P., Rybnikář, F., Chiba, T. & Inoue, T. Spinodal decomposition and succeeding crystallization in PCL/SAN blends. *Polymer* **40,** 1459–1463 (1999).
29 Svoboda, P., Svobodová, D., Chiba, T. & Inoue, T. Competition of phase dissolution and crystallization in poly(ε-caprolactone)/poly(styrene-co-acrylonitrile) blend. *Eur. Polym. J.* **44,** 329–341 (2008).
30 Keyzlarová, L. & Sáha, P. The effect of miscibility on rheological and mechanical properties of PCL/SAN blends. *Int. Polym. Process.* **14,** 228–233 (1999).
31 Abramoff, M. D., Magelhaes, P. J. & Ram, S. J. Image processing with ImageJ. *Biophotonics Int.* **11,** 36–41 (2004).
32 Taheri, M., Morshedian, J. & Khonakdar, H. A. Effect of compatibilizer on interfacial tension of SAN/EPDM blend as measured via relaxation spectrums calculated from palierne and choi–schowalter models. *Polym. Bull.* **66,** 363–376 (2011).
33 Debye, P. & Bueche, A. M. Scattering by an inhomogeneous solid. *J. Appl. Phys.* **20,** 518–525 (1949).